The Iraqi Journal For Mechanical And Material Engineering, Vol.20, No2, June.2020

THEORETICAL STUDY OF THE CONVENTIONAL AND MODIFIED SOLAR STILL

Sabah Tarik Ahmed **Hussein Hayder Mohammed Ali**
sabahsmrm@yahoo.com **me.20171@uotechnology.edu.iq**
University of Technology / Mechanical. Eng. Dept

ABSTRACT

The fresh water reserves on the earth are finite. The brackish water can be converted to the fresh water by solar water distillery. A theoretical investigation to investigate the effect of the turning hollow-cylinder within the solar still equipped with flat plate solar water collector on the output of distillate water and its thermal efficiency. The numerical analysis was carried out by using FORTRAN 90, program. The numerical analysis is used for complex phenomena without resorting to expensive prototypes and difficult experimental measurements. The study considered several parameters which are; solar radiation intensity, ambient air temperature, ambient wind velocity, basin plate temperature, basin water temperature, glass cover temperature and hollow cylinder surfaces temperature. The cumulative of distillate water output from the modified solar still increased compared with the conventional solar still by a factor not less than 240%.

KEY WARDS: Conventional; Modification Solar Water Distillery; Turning Hollow Cylinder.

دراسة نظرية لمقطر الماء الشمسي التقليدي والمعدل

صباح طارق احمد **حسين حيدر محمد علي**

الخلاصة

احتياطي المياه العذبة على الأرض تكون بكميات القليلة. يمكن تحويل المياه المالحة إلى المياه العذبة عن طريق مقطر الماء الشمسي. يتضمن البحث النظري دراسة تأثير تدوير الأسطوانة المجوفة داخل مقطر الماء الشمسي واعتمدت الدراسة على إنتاجية الماء المقطر والكفاءة الحرارية. تم إجراء التحليل العددي بواسطة برنامج فورترن 90. استخدمت التحليل العددي للظواهر المعقدة دون اللجوء إلى النماذج الأولية باهظة الثمن والقياسات التجريبية الصعبة. وكانت عدد من المتغيرات هي؛ شدة الإشعاع الشمسي ، درجة حرارة الهواء المحيط ، سرعة الرياح المحيطة ، درجة حرارة صفيحة الحوض ، درجة حرارة ماء الحوض ، درجة حرارة الغطاء الزجاجي ودرجة حرارة أسطح الأسطوانة المجوفة. زادت انتاجية مقطر الشمسي المعدل مقارنة مع مقطر الشمسي التقليدي بعامل لا يقل 240%.

الكلمات المفتاحية : التقليدي؛ المعدل ؛ مقطر الماء لشمسي؛ اسطوانة المجوفة الدواره.

Received : 10 - 7- 2019
Accepted : 8- 9 - 2019

NOMENCLATURE

Symbol	Description	Unit
A	Area	m^2
Cp	Specific heat	J/kg.K
d	Diameter	m
g	Gravitational acceleration	m/s^2
h	Convection heat transfer coefficient	$W/m^2.K$
I	Solar radiation	W/m^2
K	Thermal conductivity	W/m.K
L	Length	M
m	Mass	kg
n	Number of days in the year	-
N	Number of revolutions	rpm
P	Pressure	Pa
r	Radius	m
R	Resistance	$m^2.K/W$
t	Time	sec
T	Temperature	^oC
th	thickness	m
u	Velocity	m/s
Greek symbols:		
α	fractional solar flux absorbed	-
v	Kinematic viscosity	m^2/s
ε	Emittance of the surface	-
η	Efficiency	%
α'	Thermal diffusivity	m^2/s
∅	Latitude angle	o
Δ	Difference	-
β	Angle of tilt	o
β'	Volumetric coefficient of expansion	1/K
γ	Azimuth angle	o
θ	Contact angle	o
ρ	Density	kg/m^3
σ	Stefan-Boltzmann constant	$W/m^2.K^4$
Subscript:		
a	Air	
amb	Ambient	
ave	Average	
b	Bottom	
bp	Basin plate	
bw	Basin water	
c	Conventional solar still	
C	Convection	
D	Daily	
E	Evaporation	
ew	Cumulative distillate water output	
f	Film	
fg	Latent heat of evaporation	
g	Glass cover	
h	Hourly	
h.c	Hollow cylinder	
i	At any time	

in	Inner
ins	Insulation
j	At any element
L	Loss
m	Modified solar still
n	At any location
o	Outer
p	Plate
p.s.c	Plate solar collector
R	Radiation
s.c	Solar collector
s.d	Solar distillery
sh	Hollow cylinder shadow
su	Submerged area of a hollow cylinder in the basin water
T	Tilted surface
total	Total
u	Useful energy

INTRODUCTION

The water reserves on the earth are vast. There is only 2.5 % are in the form of drinking water, and the remains being brackish water. The brackish water can be converted to the drinking water supply by solar water distillery. A solar still characteristics as possible as clean, easy and cheap Malik [1985]. Singh [2011] conducted an experimental study in a solar still coupled with an evacuated tube collector. It also ensures the operation of the system during periods of low sunshine or cloudy condition due to the continuance of the evaporation process in these periods. The distillery productivity increases by up to 120% when combined with a solar water heater. Also, the ambient conditions are found to have a direct effect on the productivity of the distillery. The production in the night in the absence of solar radiation contributes up to 14% of the daily output due to the availability of hot water as basin water with the integration of a solar water heater. Badran [2011] compared theoretical studies with experimental data of the performance of active single slope solar still by using different operational parameters for validation purposes. The thermal performance of a single slope solar distillery coupled with collector is evaluated through implementing the following effective parameters; a) solar intensity and b) temperature differences between the distillery cover and water. Malaeb et al. [2016] enhanced distillery with a rotating cylinder are educated analytically to amend performance. The governing equations are resolved numerically and the model is calculated and validated by using experimental data. They found that the limiting speed should vary between 0.25 and 0.5 rpm depending on the specific climate conditions. In that context, a theoretical investigation is to be conducted in order to validate the optimum production by the turning hollow cylinder according to solar radiation intensity. This hollow cylinder is introduced into a solar water distillery. When solar intensity becomes high, then increase the turning of the hollow cylinder, and when solar intensity becomes low, then decrease very slowly the turning of the hollow cylinder. As it turns, a thin film of water is formed around its circumference (both the internal and external) and this film easily evaporates due to the high temperature of the hollow cylinder surface, which is fabricated of a cheap sustainable heat absorbing the material.

THEORETICAL MODEL

In this study, the procedure of theoretical solution for the double slope solar still amended by a turning hollow – cylinder. As shown in schematic diagram Figure (1), the experimental rig used in this investigation, consists of a controlled water tank supply to the double slope solar water distillery, then to the solar flat plate water collector. The purpose of such connection is to preheat the basin water of the solar still distilling before the process begins. Gravity will let the water flow from the supply water tank to the double slope distillatory and to the collector. A small water pump is used to circulate water through the solar flat plate

water collector and the basin water of the solar water distillery. The circulation of water is necessary to overcome the friction losses in pipes, so the basin water of the solar still is considered as another storage tank to the solar flat plate water collector. The DC motor interface with drive controller circuit, which consists of a variable resistance volume switch to provide the necessary current and voltage to drive the DC motor which can be powered by charge controller, battery and photovoltaic panel. A Photovoltaic of (12 V DC) with a peak power (150 W), was used for supplying electric power to the charge controller. The use of battery requires the installation of another essential element called the solar charge controller. A battery was uninterruptible power supply used for supplying electric power to the drive controller DC motor and water pump special at absent solar radiation. The power consumption of DC motor is (2.16 W) and pump is (5.52 W). In the present work, for the conventional solar still the basin water height is (1 cm), and (2 cm) for the modified solar still was selected as a compromise quantity of water adheres to the two surfaces of a hollow cylinder. The turning hollow cylinder speed of 1 rpm was selected as the best possible rotation. The following numerical analysis is used for complex phenomena without resorting to expensive prototypes and difficult experimental measurements. FORTRAN 90 programming language is used to carry out the theoretical calculations. To drive a theoretical model for the system, we need to balance the heat at each component in this system.

The Solar Water Distillery

Energy balance equations of the solar still for glass cover, heat and mass transfer occur at the interface of the outer and inner turning hollow cylinder surfaces, basin water and basin plate; mainly evaporation, convection, radiation and conduction, which are as shown in Figure(2)

The assumptions are as follows:

1- The solar distillery unit is vapor and water leakage proof.
2- Dust and dirt on a glass cover of the solar still are negligible.
3- Uniform temperature and water film thickness along each hollow cylinder element.
4- The solar still is perfectly insulated in addition to including connecting pipes.
5- Energy transformation is balanced between the water film temperature and the surface of the turning hollow cylinder temperature, hence energy equilibrium is assumed.

The Basin Plate

The rate of energy absorbed is equal to the rate of energy of stored, rate of energy of transferred to basin water and rate of energy lost through bottom and sides of the distillery: -

$$\alpha_{bp}(1-\alpha_g)(1-\alpha_w)*(A_{bp}-A_{sh})*I(t)=m_{bp}*Cp_{bp}\left(\frac{dT_{bp}}{dt}\right)+h_{C_{bp-bW}}*A_{bp}*\left(T_{bp}-T_{bw}\right)+h_{b_{bp-amb}}*A_{bp}*\left(T_{bp}-T_{amb}\right) \quad (1)$$

Where: (α_{bp}) is fractional solar flux absorbed by the basin plate, (α_g) is fractional solar flux absorbed by the glass cover, and (α_w) is fractional solar flux absorbed by the basin water, I(t) is intensity of solar radiation (W/m^2), A_{bp} is the area of basin plate (m^2), (A_{sh}) is the area of a hollow cylinder shadow (m^2), m_{bp} is the mass of the basin plate (kg), Cp_{bp} the specific heat of basin plate (J/kg.K), T_{bp} is the temperature of the basin plate (^{o}C), T_{bw} is the temperature of the basin water (^{o}C), $h_{C\,pb\text{-}bw}$ is the convection heat transfer coefficient between the basin plate and basin water which is obtained as Medugu and Ndatuwong [2009]:-

$$h_{C_{bP-bw}}=\frac{\overline{Nu}_L*K_w}{L_{Pb}} \quad (2)$$

Where

$$\overline{Nu}_d=\begin{cases}0.54(Ra_L)^{\frac{1}{4}} & (10^4\le Ra_L\le 10^7)\\ 0.15(Ra_L)^{\frac{1}{3}} & (10^7\le Ra_L\le 10^{11})\end{cases} \quad (3)$$

$$Ra_L=\frac{g*\beta'_w*(T_{bp}-T_{bw})*{L_{bp}}^3}{\upsilon_w*\propto'_w} \quad (4)$$

Where: υ_w, α_w, and β'_w are the kinematic viscosity (m^2/sec), thermal diffusivity $\{\propto'_w=\frac{k_w}{\rho_w*Cp_w}\left(\frac{\mathrm{m}^2}{sec}\right)\}$, and the thermal expansion coefficient of basin water $\{\beta'_w=\frac{1}{T}\left(\frac{1}{K}\right)\}$, respectively. K_w is thermal

conductivity (W/m.K) also, the ratio of surface area to perimeter of the basin plate represents L_{bp} (m). The convection heat transfer coefficient between the basin plate and basin water (W/m^2. K).

$h_{b_{bp-amb}}$ represents the heat transfer coefficient from the bottom basin plate to ambient air and it is given by:-

$$h_{b_{bp-amb}} = \frac{1}{\frac{k_{ins}}{L_{ins}} + \frac{1}{hrc_{b-amb}}} \quad (5)$$

Where k_{ins} is insulation thermal conductivity (W/m. K) and L is thickness of insulation (0.05 m). $h_{RC\ b-amb}$ represents the convection and radiation heat transfer coefficient to the environment in (W/m^2. K) is expressed as Medugu and Ndatuwong [2009]:-

$$h_{RC_{b-amb}} = 5.7 + 3.8u_{amb} \quad (6)$$

Where u_{amb} is the wind ambient air velocity in (m/s)

The turning hollow cylinder

The quantity of transient heat transfer between elements of the hollow cylinder surfaces and the surrounding air at the inner and outer surfaces of the hollow cylinder becomes:

$$\alpha_{hc} * (1 - \alpha_g) * I(t) = \frac{d}{dt}\left[m_{hc} * Cp_{hc} * T_{hc} + m_{wf} * Cp_{wf} * T_{wf}\right] + k_{hc}\left(\frac{T_{hc} - T_{hc-before}}{th_{hc}}\right) + k_{hc}\left(\frac{T_{hc-after} - T_{hc}}{th_{hc}}\right) + \left[h_{C_{hco-gin}} + h_{E_{hco-gin}} + h_{R_{hco-gin}}\right](T_{hco} - T_{gin}) + [h_{C_{hci-gin}} + h_{E_{hco-gin}}](T_{hcin} - T_{gin}) \quad (7)$$

Where: (α_{hc}) is the fractional solar flux absorbed by the hollow cylinder plate, (α_g) is the fractional solar flux absorbed by the glass cover, I(t) is intensity of solar radiation (W/m^2), m_{hc} is the mass of the hollow cylinder element (kg/m^2) for a given time period dt (sec), Cp_{hc} the specific heat of hollow cylinder (J/kg. K), T_{hc} is the temperature of the hollow cylinder element (^{o}C), m_{wf} the mass of water film along this element (kg/m^2), and Cp_{wf} the specific heat of water (J/kg.K). k_{hc} is the thermal conductivity of the hollow cylinder (W/m.K), T_{wf} is the temperature of the water film element and is assumed that ($T_{wf} = T_{hc}$), t_{hc} is the thickness of the hollow cylinder element (0.001m), The terms given before and after elements referring to the two elements strip of the hollow cylinder that are in direct contact with the element under consideration as illustrated in Figure(3). $h_{Chco\text{-}gin}$ is the convection heat transfer coefficient between the hollow cylinder element outside and inner the surface of the glass cover (W/m^2.K). $h_{Ehco\text{-}gin}$ is the evaporation heat transfer coefficient between the hollow cylinder element outside and inside the glass cover (W/m^2.K). $h_{Rhco\text{-}gin}$ is the radiation heat transfer coefficient between the hollow cylinder element outside and the inside glass cover (W/m^2.K). $h_{Chcin\text{-}gin}$ is the convection heat transfer coefficient between the hollow cylinder element inside and inner the surface of the glass cover (W/m^2.K). $h_{Ehcin\text{-}gin}$ is the evaporation heat transfer coefficient between the hollow cylinder element inside and inside the glass cover in (W/m^2 . K) Medugu and Ndatuwong [2009]:-

$$h_{C_{hco-gin}} = 0.884\left[(T_{hco} - T_{gin}) + \frac{(P_{hco} - P_{gin}) * (T_{hco} + 273)}{(2.689 * 10^5 - P_{hco})}\right]^{1/3} \quad (8)$$

The pressures have been calculate by means of the expression in (Pa) Fernandez and Norberto [1990]:-

$$P_{gi} = e^{\left(25.317 - \frac{5144}{(T_{gin} + 273)}\right)} \quad (9)$$

$$P_{hco} = e^{\left(25.317 - \frac{5144}{(T_{hco} + 273)}\right)} \quad (10)$$

The evaporation heat transfer coefficient between the hollow cylinder element inside and the outer surface of the glass cover is given by Medugu and Ndatuwong [2009]:-

$$h_{E_{hco-gin}} = 16.273 * 10^{-3} * h_{C_{hco-gin}} * \frac{(P_{hco} - P_{gin})}{(T_{hco} - T_{gin})} \quad (11)$$

The radiation heat transfer coefficients between the hollow cylinder element outside and the inner surface of the glass cover is given by Incropera [2005]:-

$$h_{R_{hco-gin}} = \frac{\sigma}{\frac{1}{\varepsilon_{hco}}+\frac{1}{\varepsilon_{gi}}-1}\left[\left(T_{gi}+T_{hco}+546\right)*\left(\left(T_{gi}+273\right)^2+\left(T_{hco}+273\right)\right)^2\right] \quad (12)$$

Where σ is the Stefan-Boltzmann constant (W/m^2.K^4), ε_{hco} is the emittance of the hollow cylinder element outside and $\varepsilon_g$is the emittance of the glass.

The convection heat transfer coefficient between the hollow cylinder element inside and the inner surface of the glass cover is given by Medugu and Ndatuwong [2009]:-

$$h_{C_{hcin-gin}} = 0.884\left[\left(T_{hcin}-T_{gi}\right)+\frac{\left(P_{hcin}-P_{gi}\right)*\left(T_{hcin}+273\right)}{\left(2.689*10^5-P_{hcin}\right)}\right]^{1/3} \quad (13)$$

Where $P_{hcin} = e^{\left(25.317-\frac{5144}{\left(T_{hcin}+273\right)}\right)}$ (14)

The evaporation heat transfer coefficient between the hollow cylinder element inside and the inner surface of the glass cover is given by Medugu and Ndatuwong [2009]:-

$$h_{E_{hcin-gin}} = 16.273*10^{-3}*h_{C_{hcin-gin}}*\frac{\left(P_{hcin}-P_{gin}\right)}{\left(T_{hcin}-T_{gin}\right)} \quad (15)$$

The Basin Water

The rate of energy absorbed from the sun, flat plate solar water collector and the rate of energy convection from the basin plate is equal to the rate of energy stored and rate of energy transferred to the glass cover:

$$Q_u+\alpha_w\left(1-\alpha_g\right)*\left(A_{bp}-A_{sh}\right)*I(t)+h_{C_{bp-bW}}*A_{bp}*\left(T_{bp}-T_{bw}\right)=m_{bw}*Cp_w*\left(\frac{dT_{bw}}{dt}\right)+\left[h_{R_{bw-gin}}+h_{C_{bw-gin}}+h_{E_{bw-gin}}\right]*\left(A_{bp}-A_{su}\right)*\left(T_{bw}-T_{gi}\right) \quad (16)$$

Where: Q_u is the useful heat from flat plate solar water collector (W), α_w is fractional solar flux absorbed the basin water surface, α_g is the cover absorbance, I is the solar radiation (W/m^2), $h_{Cbp\text{-}bw}$ is the convection heat transfer coefficient between the basin plate and the basin water which is obtained from equation (2) in (W/m^2. K), T_{bp} is the basin plate temperature (^{o}C), T_{bw} is the basin water (^{o}C). m_{bw} is the mass of the water in the solar still (kg), Cp_w is the heat capacity of the basin water (J/kg.^{o}C), T_{gi} is the temperature of the inside surface of the glass cover (^{o}C). $h_{R_{bw-gin}}$ is the radiation heat transfer coefficient between the basin water and the inner surface of the glass cover (W/m^2.K). $h_{C_{bw-gin}}$ is the convection heat transfer coefficient between the basin water and the inside glass cover (W/m^2. K). $h_{E_{bw-gin}}$ is the evaporation heat transfer coefficient between the basin water and the inside glass cover (W/m^2 .K). (A_{su}) is the submerged area of a hollow cylinder in the basin water (m^2).

The radiation heat transfer coefficients between the basin water and the inner surface of the glass cover is given by Incropera [2005]:-

$$h_{R_{bw-gi}} = \frac{\sigma}{\frac{1}{\varepsilon_{bw}}+\frac{1}{\varepsilon_{gi}}-1}\left[\left(T_{bw}+T_{gin}+546\right)*\left(\left(T_{bw}+273\right)^2+\left(T_{gin}+273\right)^2\right)\right] \quad (17)$$

Where ε_{bw} is the emittance of the basin water and $\varepsilon_g$is the emittance of the glass.

The convective heat transfer coefficient between the basin water and the inner surface of the glass cover is given by Medugu and Ndatuwong [2009]:

$$h_{C_{bw-gin}} = 0.884\left[\left(T_{bw}-T_{gin}\right)+\frac{\left(P_{bw}-P_{gin}\right).\left(T_{bw}+273\right)}{2.689*10^5-P_{bw}}\right]^{1/3} \quad (18)$$

The pressures have been calculate by means of the expression in (Pa) Fernandez and Norberto [1990]:-

$$P_{bw} = e^{\left(25.317-\frac{5144}{\left(T_{bw}+273\right)}\right)} \quad (19)$$

The evaporative heat transfer coefficients between the basin water and the inner surface of the glass cover are respectively given by Medugu and Ndatuwong [2009]:-

$$h_{E_{bw-gi}} = 16.273*10^{-3}*h_{C_{bw-gin}}*\frac{\left(P_{bw}-P_{gin}\right)}{\left(T_{bw}-T_{gin}\right)} \quad (20)$$

The Glass Cover Distillery

Energy balance equations of the glass cover for the modification of the solar still as following:-

The Inner Glass Cover Surface:

The rate of energy fractional solar flux absorbed from sun, the rate of energy (radiation, convection and evaporation) from the basin water, the rate of energy (radiation, convection and evaporation) from the outer hollow cylinder surface, and the rate of energy (convection and evaporation) from the inner hollow cylinder surface is equal to the rate of energy stored and rate of energy transferred from the inner to outer of the glass cover as following:-

$$\alpha_g * I(t) * A_g + \left[h_{R_{bw-gin}} + h_{C_{bw-gin}} + h_{E_{bw-gin}}\right] * \left(A_{bp} - A_{su}\right) * \left(T_{bw} - T_{gin}\right) + \left[h_{R_{hco-gin}} + h_{C_{hco-gin}} + h_{E_{hco-gin}}\right] * \left(A_{j_{hc}}\right) * \left(T_{hco} - T_{gin}\right) + \left[h_{C_{hcin-gin}} + h_{E_{hcin-gin}}\right] * \left(A_{j_{hc}}\right) * \left(T_{hcin} - T_{gin}\right) = m_g * Cp_g * \frac{dT_g}{dt} + \frac{K_g}{th_g} * \left(T_{gin} - T_{go}\right) \quad (21)$$

Where α_g is the fractional solar flux cover absorbance, I is the solar radiation (W/m^2), A_g is the glass cover area (m^2). m_g is the mass of glass cover (kg), Cp_g is the heat capacity of the glass cover (J/kg.K), T_{go} is the outer glass cover surface temperature(^{o}C). K_g is thermal conductivity (W/m.K) and th_g is the thickness of glass cover (0.004m).

$A_{j_{hc}}$ is the element area of the hollow cylinder surface that interacts with the glass cover (m^2) and each element (j) of the n hollow cylinder elements surfaces are of width dz and length Lhc and they are (1.22 m) each. The area is given by:-

$$A_{j_{hc}} = L_{hc} \sum_{j=1}^{n} dz \quad (22)$$

The time step used to be 0.5 sec as this amount gave a sensible calculation time and the use of smaller time steps barely affected the results but conspicuously increased the calculation time. The properties of humid air, i.e. (thermal conductivity, thermal diffusivity, specific heat capacity, density, saturated vapor pressure, and viscosity) are taken as Tsilingiris [2008]. In building the simulation prototype for the amended solar water distillery, both the basin water in the solar still and glass cover were treated as one unit with a uniform temperature distribution, while the hollow cylinder was deliberate into longitudinal elements for which a governing balance equation was written based on the location of these elements as the hollow cylinder turning. Four segments were well-known in Figure(3) along the perimeter of the hollow cylinder for receiving altered amount of sun rays depending on the particular location at a certain time, as shown in Figure (2). For a given time period dt (sec), the length of the incremental distance dz (m) was intended as:

$$dz = \frac{2*\pi*r*dt}{60*N_{hc}} \quad (23)$$

Where N_{hc} is the number of revolutions per minute of the hollow cylinder (rpm) and r is the radius of the hollow cylinder (m).

The Outer Glass Cover Surface:

The rate of energy conduction from the inner glass cover is equal to the rate of energy convection and radiation transferred to the ambient air as following; -

$$\frac{K_g}{th_g} * \left(T_{gin} - T_{go}\right) = \left[h_{C_{gin-amb}} + h_{R_{gin-amb}}\right] * \left(T_{go} - T_{amb}\right) \quad (24)$$

Where $h_{C_{gin-amb}}$ is the convection heat transfer coefficient between outer surface glass cover and ambient in (W/m^2. K) is expressed as Duffie [1980]:-

$$h_{C_{gin-amb}} = 2.8 + 3u_{amb} \quad (25)$$

Where u_{amb} is the wind air velocity in (m/s); and $h_{R_{gin-amb}}$ is the radiation heat transfer coefficient from the outer surface glass cover accounts for radiation exchange with sky at T_{sky}. For convenience, we reference this radiation exchange to the ambient temperature (T_{amb}), so that the radiation heat transfer coefficient can be written as Incropera [2005]:-

$$h_{r,b-a} = \sigma * \varepsilon_{go} * \left[\left(T_{amb} + T_{go} + 546\right) * \left((T_{amb} + 273)^2 + (T_{go} + 273)^2\right)\right] \quad (26)$$

ε_{go} is the emittance of the outer surface glass cover.

The Water Film Thickness

The water film thickness around inner and outer surfaces of a turning hollow cylinder assuming that at the point the cylinder leaves the liquid, it can be approximated to a flat surface remote at the same angle of contact. The dimensionless uniform thickness th_{wf0} could then be determined as a function of the contact angle Θ_c, a dimensionless capillary number and fluid property number. With the intention of extend this theory from flat plate analysis to a turning hollow cylinder, the measurement position Θ_j was accounted for and the water film thickness at the top of the hollow cylinder th_{wft} (m) could be first calculated as a function of th_{wf0} and then the film thickness th_{wf} (m) at a given measurement position around its circumference could be determined Tharmalingam and Tarawneh [1978]:-

$$th_{wft} = th_{wf} - \frac{\rho_w * g * th_{wf}^3 * sin\Theta_j}{3 * \mu_w * u_{hc}} = th_{wf0} - \frac{\rho_w * g * th_{wf0}^3 * sin\Theta_c}{3 * \mu_w * u_{hc}} \quad (27)$$

Where ρ_w is the density of water (kg/m^3), μ_w is the dynamic viscosity of water (kg/m.sec) and u_{hc} is the perimeter velocity of the hollow cylinder which have been calculate by means of the expression in (m/s):-

$$u_{hc} = \frac{2 * \pi * r * N_{hc}}{60} \quad (28)$$

Hourly cumulative distillate water output for the solar water distilleries

Conventional Solar Water Distillery

The hourly cumulative distillate water output, m_{ewc}, for the conventional solar still in (Kg/m^2.hr) was obtained by the evaporation heat transfer coefficient $h_{E_{bw-gin}}$, multiplied by difference between basin water temperature T_{bw} (^{o}C) and inner glass cover temperature T_{gin} (^{o}C) and 3600, hence the results were divided by the average latent heat h_{fg} at average basin water temperature:

$$m_{ewc} = \frac{h_{E_{bw-gin}} * A_{bp} * (T_{bw} - T_{gin})}{h_{fg}} * 3600 \quad (29)$$

Where A_{bp} is the basin plate area as (1 m^2) and h_{fg} is the average latent heat in (J/Kg) is obtained by Kabeel and Abdelgaied [2016]:-

$$h_{fg} = 10^3[2501.9 - 2.40706 * T_{bw} + 1.192217 * 10^{-3} * T_{bw}^2 - 1.5863 * 10^{-5} * T_{bw}^3] \quad (30)$$

Modified Solar Water Distillery

The hourly cumulative distillate water output, m_{ewm}, for the modified solar stillin (kg/m^2.hr) was obtained by the evaporation heat transfer coefficients $h_{E_{bw-gin}}$, $h_{E_{hco-gin}}$ and $h_{E_{hci-gin}}$ multiplied by difference between parameters temperatures and inner glass cover temperature T_{gin} (^{o}C) and 3600, hence the results were divided by the average latent heat h_{fg} at average basin water temperature:-

$$m_{ewm} = \left[\frac{h_{E_{bw-gin}} * (0.8012 A_{bp}) * (T_{bw} - T_{gin}) + h_{E_{hco-gin}} * A_{j_{hc}} * (T_{hco} - T_{gin}) + h_{E_{hci-gin}} * A_{j_{hc}} * (T_{hcin} - T_{gin})}{h_{fg}}\right] * 3600 \quad (31)$$

Hourly efficiency of the solar water distilleries

Conventional Solar Water Distillery

The hourly efficiency, $\eta_{h.c.}$, for the conventional solar still was obtained by the hourly cumulative distillate water output m_{ewc}, multiplied by the average latent heat h_{fg} at average basin water temperature T_{bw} (^{o}C), hence the results were divided by the daily average solar radiation I(t) (W/m^2) over the whole area A (1 m^2) and period Δt (3600 sec) of the conventional solar water distillery:

$$\eta_{h.c.} = \frac{m_{ewc} * h_{fg}}{I(t) * A_{bp} * \Delta t} * 100\% \quad (32)$$

Where: A_{bp} is the basin plate area.

Modified Solar Water Distillery

The hourly efficiency, $\eta_{h.m.}$, for the modified solar stillwas obtained by the cumulative distillate water output m_{ewm}, multiplied by the average latent heat h_{fg} at average basin water temperature T_{bw} (^oC), hence the results were divided by the daily average solar radiation I(t) (W/m^2) over the whole area A (m^2) and period Δt (3600 sec) of both the modified solar still and flat plate solar water collector.

$$\eta_{h.m.} = \frac{m_{ewm} * h_{fg}}{I(t) * A_{bp} * \Delta t + I_{S.C.}(t) * A_{s.c.} * \Delta t + (P_m + P_p) * \Delta t} * 100\% \quad (33)$$

Where; $I_{S.C.}$ and $A_{S.C.}$ is the solar radiation and surface area of flat plate solar water collector respectively.

Initial and Boundary Conditions

The initial and boundary conditions required to start up the numerical analysis model of the solar water distillery. It is included the initial temperatures for the basin plate (T_{bp}), basin water (T_{bw}), hollow cylinder (T_{hc}), glass cover inlet (T_{gi}) and outlet (T_{go}). Expressive the weather conditions, geometrical, operational data, initial temperatures at time zero T_{bp}^0, T_{bw}^0, T_{hc}^0, T_{gi}^0 and T_{go}^0; and boundary conditions at time zero the ambient air temperature (T_{amb}^0) and the wind ambient air velocity (u_{amb}^0). The heat balance equations were used to determine the first estimates for T_{bp}, T_{bw}, T_{hc}, T_{gi} and T_{go} in the next time step as the following:

1- Estimating the initial conditions of T_{bp}^0, T_{bw}^0, T_{hc}^0, T_{gi}^0 and T_{go}^0 then T_{bp}^1at the next time step was calculated using the energy balance equation (1) written for basin plate.
2- Estimating T_{bp}^1, T_{bw}^0, T_{hc}^0, T_{gi}^0 and T_{go}^0 then T_{bw}^1at the next time step was calculated using the energy balance equation (16) written for the basin water.
3- Estimating T_{bp}^1, T_{bw}^1, T_{hc}^0, T_{gi}^0 and T_{go}^0 then T_{hc}^1at the next time step was calculated using the energy balance equation (7) written for turning hollow cylinder, where the initial temperatures $T_{hc\ before}$ and $T_{hc\ after}$ were assumed to be equal to the initial hollow cylinder temperature.
4- Estimating T_{bp}^1, T_{bw}^1, T_{hc}^1, T_{gi}^0 and T_{go}^0 then T_{gi}^1at the next time step was calculated using the energy balance equation (21) written for inner glass cover.
5- Estimating T_{bp}^1, T_{bw}^1, T_{hc}^1, T_{gi}^1 and T_{go}^0 then T_{g0}^1at the next time step was calculated using the energy balance equation (24) written for outer glass cover.
6- The significant hollow cylinder balance equation was written for each element depending on its position Figure (2). As for the model's boundary conditions, the basin water temperature (T_{bw}) was considered to be equal to the temperature of the first hollow cylinder element (T_{hc}) leaving the water.
7- The temperature of the water film element (T_{wf}) on hollow cylinder element surface assumed that ($T_{wf} = T_{hc}$)**.**
8- The above estimating were solved iteratively using Finite Difference method in FORTRAN 90 language was written to carry out the theoretical calculations for the productivity and efficiency of the solar water distillery. The time step used was 0.5 Sec as this value gave a reasonable calculation time and the use of smaller time steps hardly affected the results but notably increased the calculation time. As illustrated in the flowchart of Figure (4).

RESULTS AND DISCUSSION

Theoretical model was done according to the schematic diagram in Figure (1). Many computational runs were performed at various ambient air temperature, wind ambient air velocity and initial conditions (basin plate temperature, basin water temperature, glass cover temperature and hollow cylinder temperature). The data from experimental work are taken to start the model as an initial and boundary conditions. Tecplot 9.0 program is used to represent the theoretical variation of temperatures, solar radiation intensity, productivity and efficiency of the solar water distillery. The variable was calculated theoretically for the period of four months on the average day from January, 2018 to April, 2018 of climatic Kirkuk city, Iraq.

Figures (5), (6), (7) and (8) show the variation of the temperatures of the basin plate, basin water, glass cover, ambient air and solar radiation intensity with time for the conventional solar still for average days of January, February, March and April. All the Fig. show the similar trends of variation. Where the temperature rises during the daytime up to the maximum value at hour 14:00, and then it decreases. These results were similar to the results of many investigators Tarawneh [2007] and Akash et al. [2000]. It is clearly that, all temperatures increase with time up to a maximum value at hour 14:00 which represent two hours' time delay with respect to solar radiation intensity maximum at hour 12:00. This is due to continuous thermal inertia after solar intensity maximum. Figures (9), (10), (11) and (12) illustrate that peak value in hollow cylinder surface temperature reached during period of 13 to 14 hour for the modified solar still due to great availability of solar radiation as well as warming of basin water by flat plate solar water collector from early morning to afternoon. It also observed that, highest temperature of turning hollow cylinder due to manufacturing from aluminum plate having compared higher thermal conductivity. It was noticed that the modified solar still operated at higher temperature than the conventional solar still due to the flat plate solar water collector, which increased the heat energy gain in a solar water distillery.

Figures (13), (14), (15) and (16) show the variation of hourly distillate water output with time for the conventional and modified solar still in different months. It is shown that, the highest hourly distillate water output is gained by the modified solar still having (auto turning hollow cylinder plus flat plate solar water collector) and least gained by conventional solar water distillery. Figures (17), (18), (19) and (20) show the variation of theoretical solar radiation intensity and amount of cumulative distillate water. It seems that the productivity of January, February, March and April were (1080, 1640, 2785, and 2910 ml/m^2.day) respectively for the conventional solar water distillery. The productivity of January, February, March and April were (3690, 6010, 9560, and 10030 ml/m^2.day) respectively for the modified solar water distillery. The cumulative of distillate water output from the modified solar still increased compared with the distillate water output from the conventional solar water distillery. The cumulative was increased by a factor not less than (240) %. These are due to the increased surface area of water evaporation and have formed thin film of water carry around its two faces of turning the hollow cylinder. It is observed that the cumulative distillate water output increases with time for both the conventional and modification solar water distillery. It also shows that the optimum cumulative distillate water output occurred in the late afternoon due to the warm basin water and ambient air temperature will overcome decreasing. The productivity of the modified solar still is higher than that of the conventional solar water distillery. This due to coupling the modified solar still with a flat plate solar water collector, also auto turning hollow cylinder involve an additional surface to capture solar radiation to warm the basin water as well as increase the surface evaporation to be distilled. These improvements lead to evaporation augmentation. These results agree with experimental results and with others Badran [2011], Sethi and Dwivedi [2013] and Malaeb et al. [2016].

Figure (21) illustrates the variation of hourly efficiency for the conventional and modified solar still on 17^{th} of January. It can be observed that the hourly efficiency increases with time till it reaches the peak value in the late afternoon. Because the incident solar radiation is larger than heat losses lead to warm basin water at this period. It also shows that the optimum hourly efficiency occurred in the late afternoon due to the warm basin water and the solar radiation intensity and ambient air temperature will overcome decreasing. Therefore, the heat losses from the glass cover to the ambient air in this time, the high condensation process will augment on the inner glass cover surface. It is seen that the optimum hourly efficiency of conventional solar still equal to (62 %), that is lower than the hourly efficiency of the modified solar still (88%). Normally the hourly efficiency of conventional solar still is less than the hourly efficiency of the modification solar water distillery. Due to the effective evaporative area of the modified solar still is larger than that in conventional solar still as well as high temperature difference occurred between the glass and basin water in the modification solar water distillery. Figures (22), (23) and (24) show the variation of hourly efficiency for the

conventional and modified solar still on average day from February to April. It can be seen from Figure (22) to Figure (24) that have similar trends were noticed for the Figure (21).

Figure (25) shows the variation of daily cumulative distillate water output for different types of solar water distillery. The Figure shows that the modified solar still of the present work gives the highest productivity when compared with Cooper [1973] and Ayoub [2014]. This due to the preheating of the water in the solar water heater before starting the water evaporation process, and also due to auto-turning of the hollow cylinder when compared with Ayoub [2014]. The present design is better due to the increasing surface area of evaporation and increase basin water temperature.

CONCLUSION

Form the results obtained from this work, the following conclusions can be made:

1- The solar still can be successfully calculated by using FORTRAN 90, with comparable results with the actual solar water distillery.

2- The cumulative of distillate water output from the modified solar still increased compared with the distillate water output from the conventional solar still by a factor not less than (240) %.

3- The optimum hourly efficiency of conventional solar still equal to (62 %), that is lower than the hourly efficiency of the modified solar still (88%).

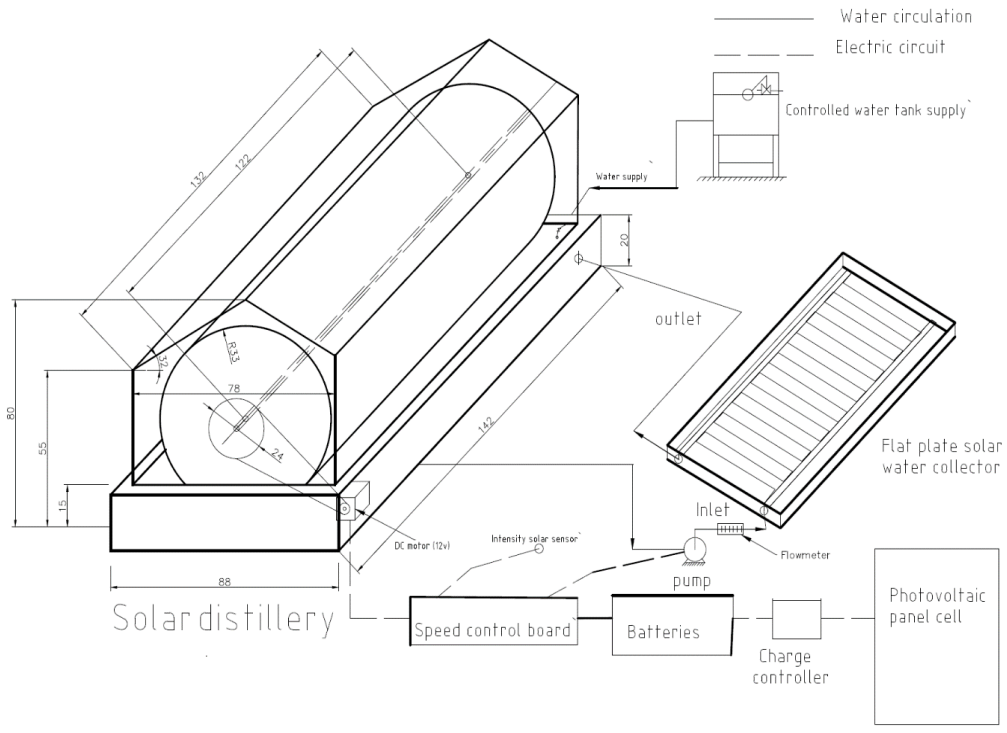

Fig. (1). Schematic diagram of rig test of the modified solar still

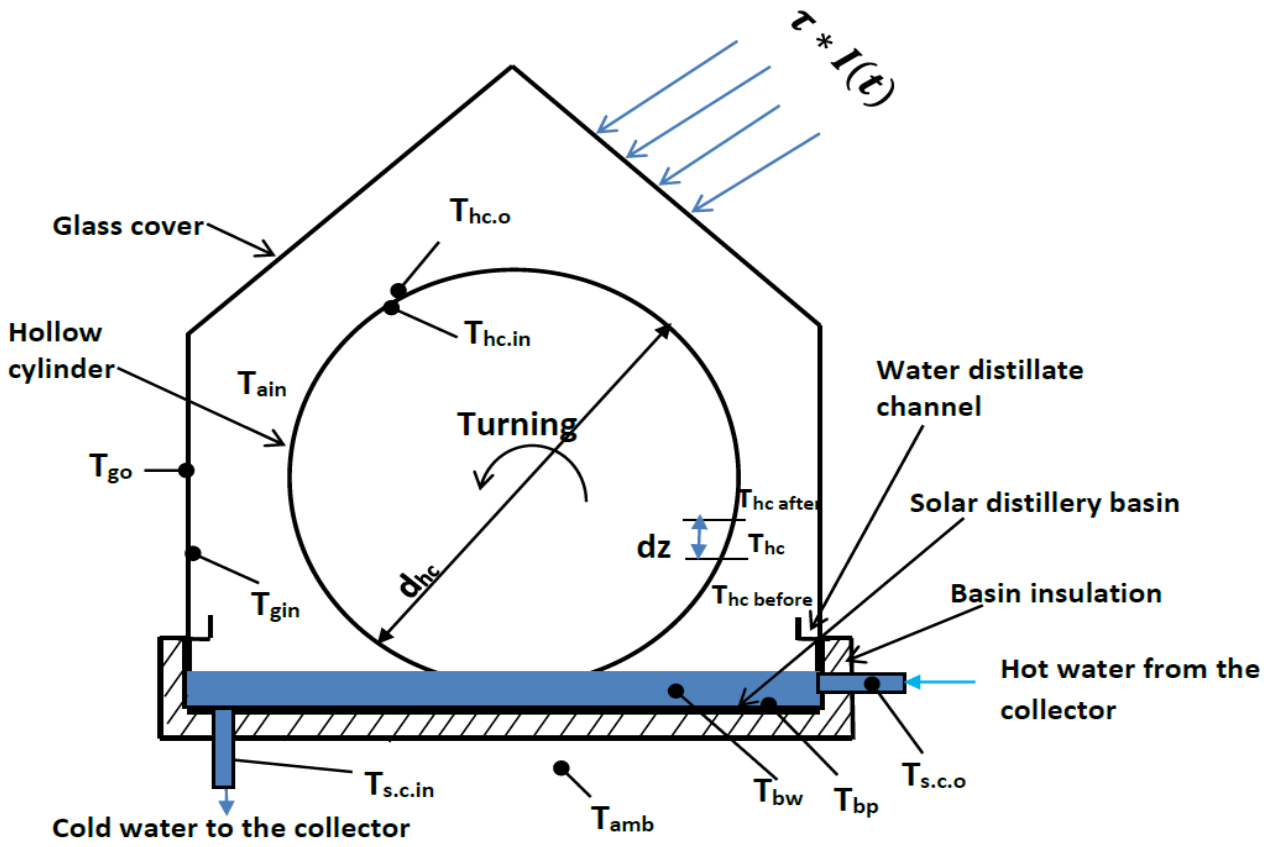

Fig. (2) show heat and mass transfer occur at the interface of the surrounding turning hollow-cylinder.

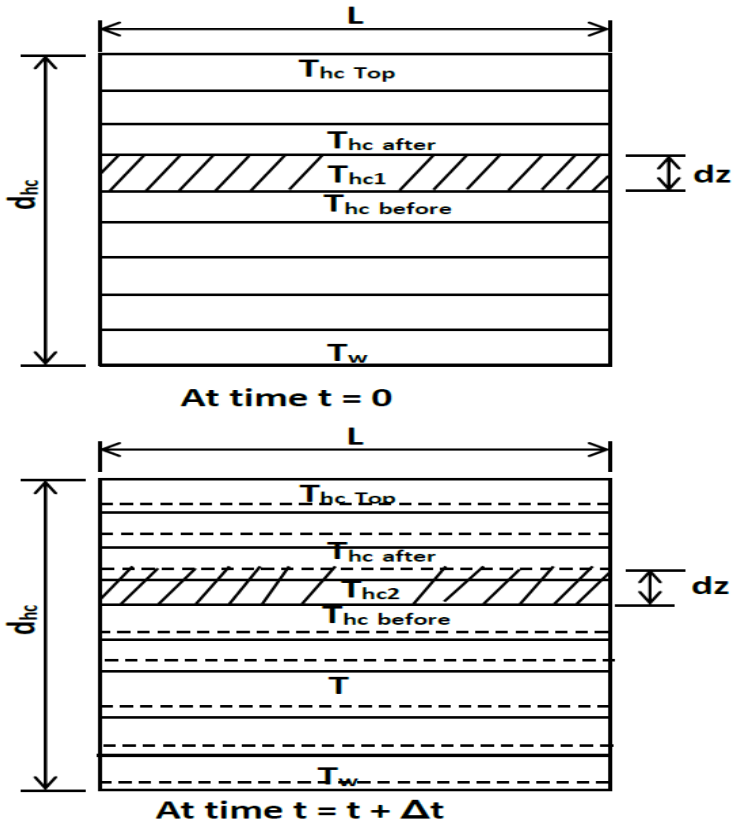

Fig. (3) Evolution of the longitudinal elements along the turning hollow cylinder with vary time.

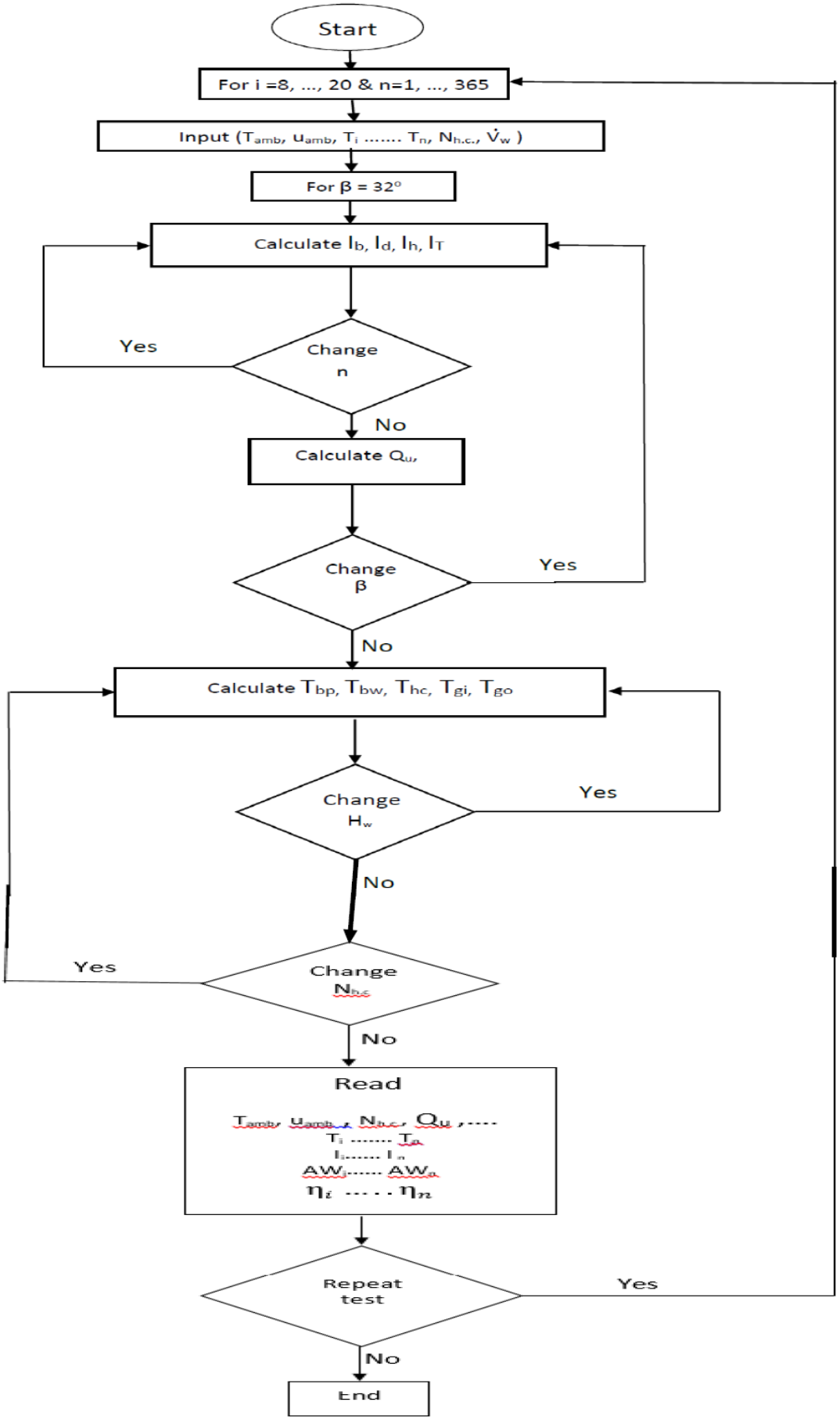

Fig. (4). Flow charts for data reader.

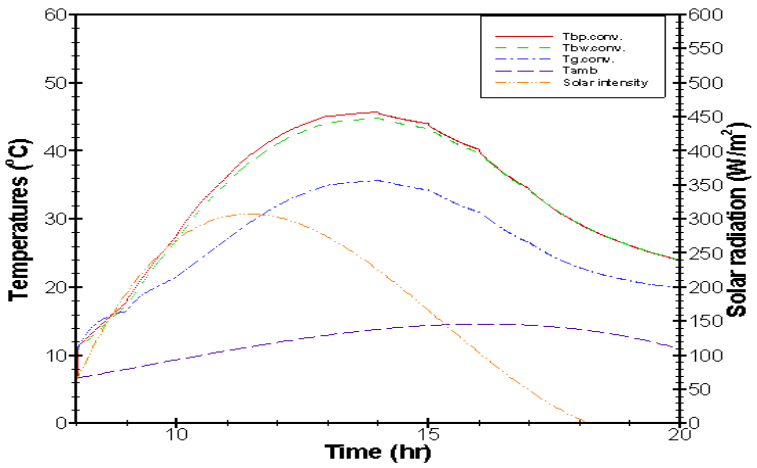

Fig. (5). Variation of solar radiation intensity and temperatures for the conventional solar still with time of the day on Jan. 17. 2018.

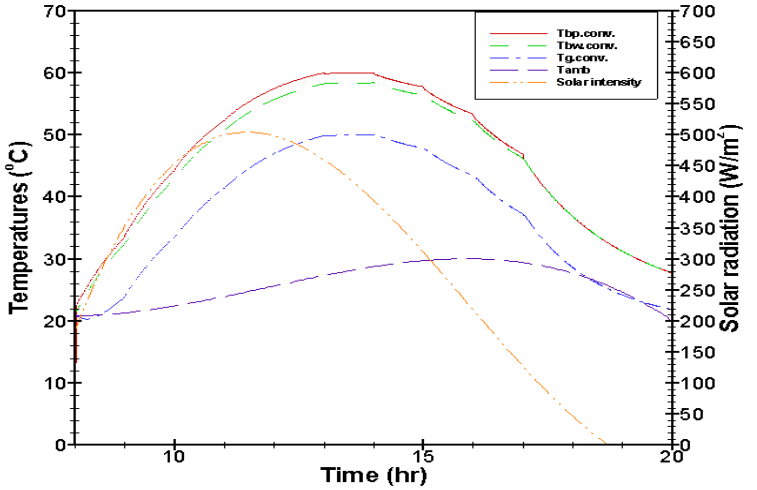

Fig. (6). Variation of solar radiation intensity and temperatures for the conventional solar still with time of the day on Feb. 16. 2018.

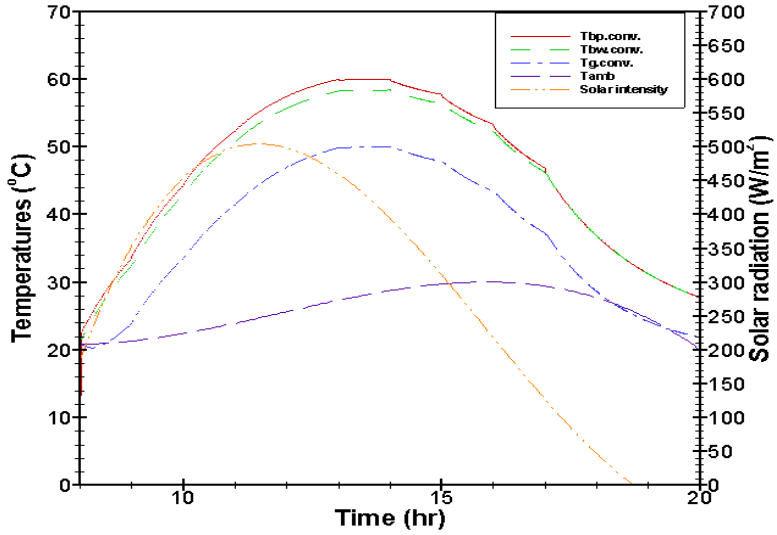

Fig. (7). Variation of solar radiation intensity and temperatures for the conventional solar still with time of the day on Mar. 16. 2018.

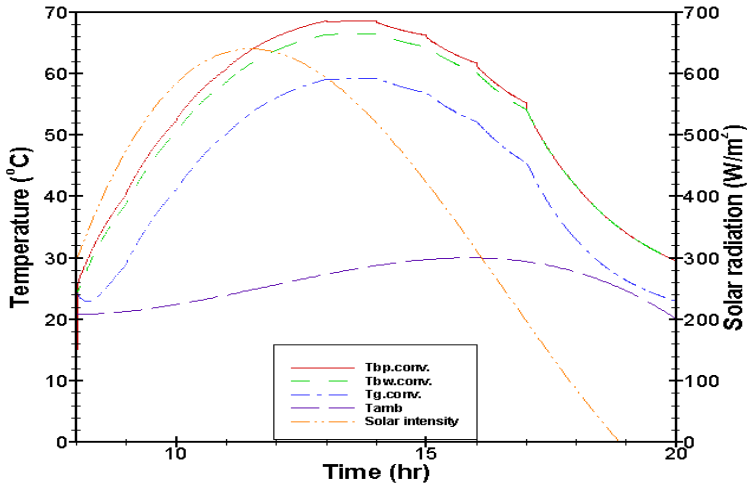

Fig. (8). Variation of solar radiation intensity and temperatures for the conventional solar still with time of the day on Apr. 15. 2018.

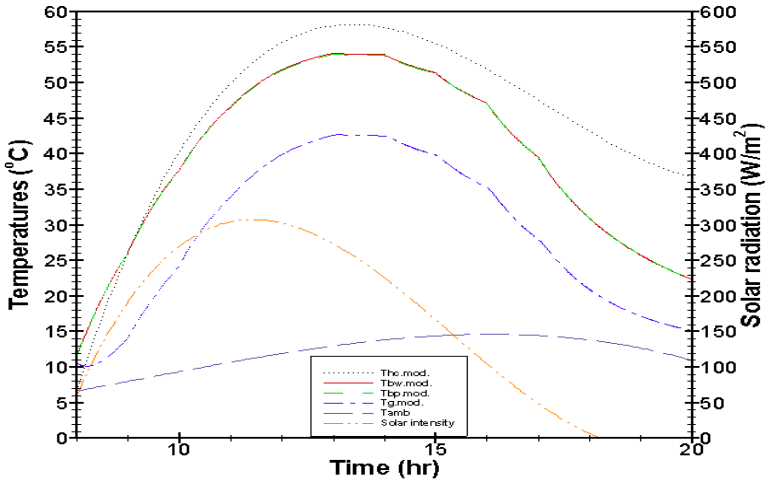

Fig. (9). Variation of solar radiation intensity and temperatures for the conventional solar still with time of the day on Jan. 17. 2018.

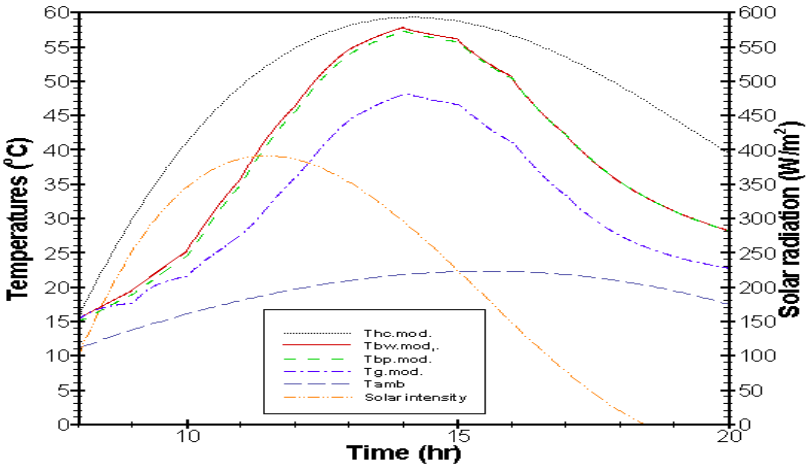

Fig. (10). Variation of solar radiation intensity and temperatures for the conventional solar still with time of the day on Feb. 16. 2018.

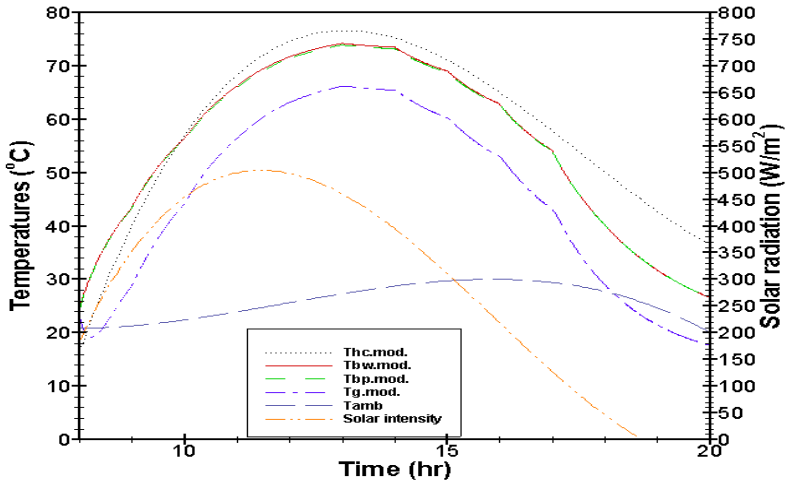

Fig. (11). Variation of solar radiation intensity and temperatures for the conventional solar still with time of the day on Mar. 16. 2018.

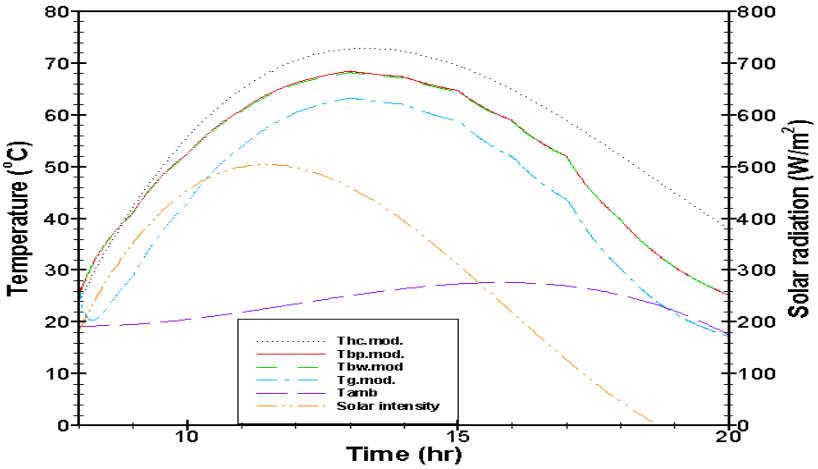

Fig. (12). Variation of solar radiation intensity and temperatures for the conventional solar still with time of the day on Apr. 15. 2018.

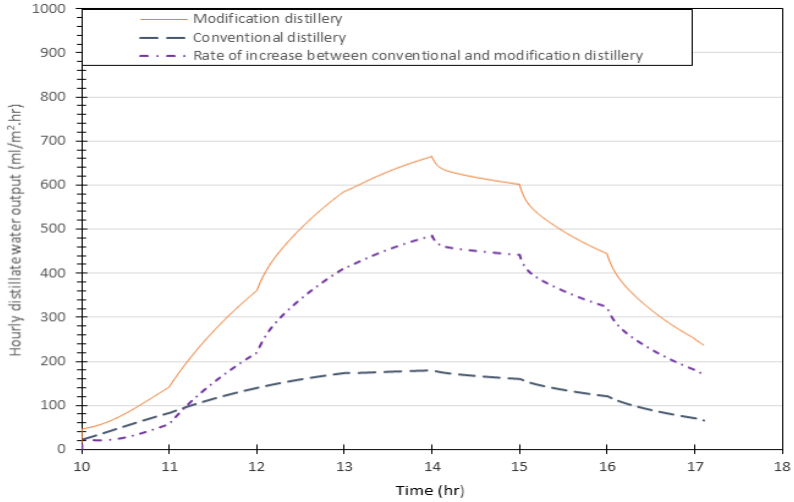

Fig. (13). Hourly variation of freshwater productivity for the conventional and modified solar still (auto turning hollow cylinder + flat plate solar water collector) on 17th Jan 2018, Kirkuk, Iraq.

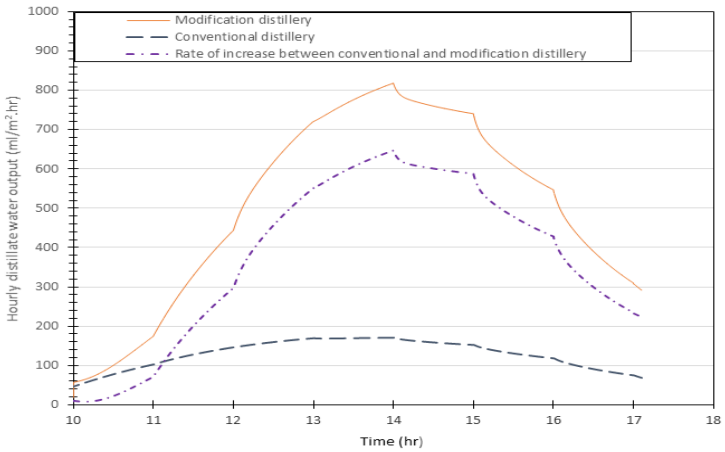

Fig. (14). Hourly variation of freshwater productivity for the conventional and modified solar still (auto turning hollow cylinder + flat plate solar water collector) on 16th Feb 2018, Kirkuk, Iraq.

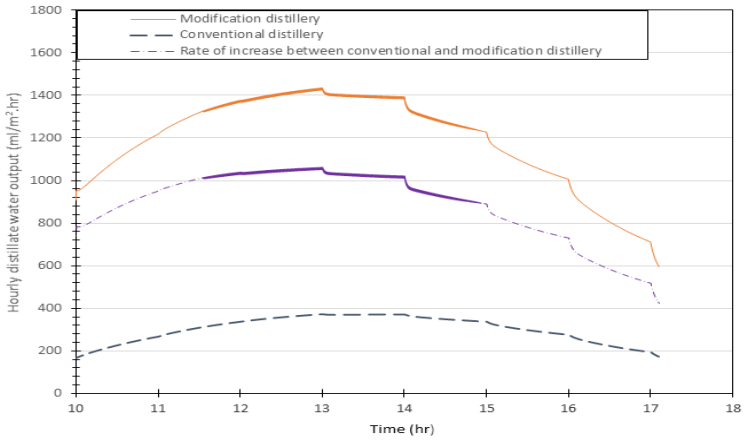

Fig. (15). Hourly variation of freshwater productivity for the conventional and modified solar still (auto turning hollow cylinder + flat plate solar water collector) on 16th Mar 2018, Kirkuk, Iraq.

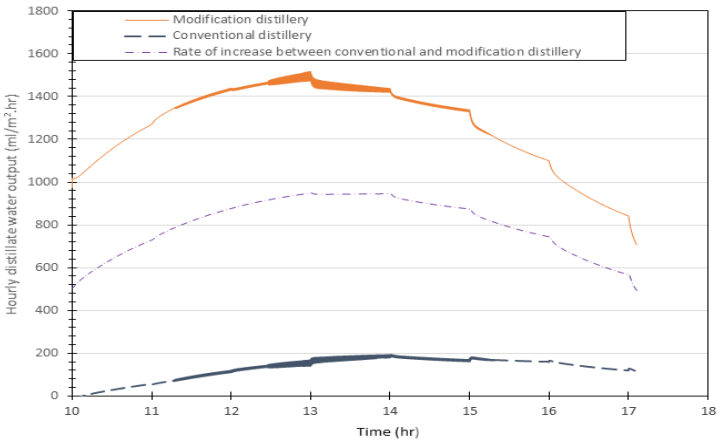

Fig. (16). Hourly variation of freshwater productivity for the conventional and modified solar still (auto turning hollow cylinder + flat plate solar water collector) on 15th Apr 2018, Kirkuk, Iraq.

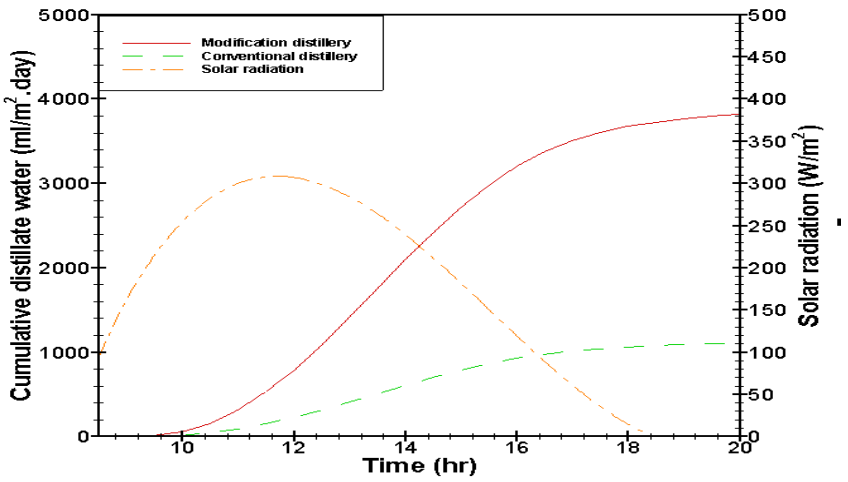

Fig. (17). Variation of theoretical solar radiation intensity and amount of cumulative distillate water for the conventional and modified solar still with time of the day on Jan. 17. 2018.

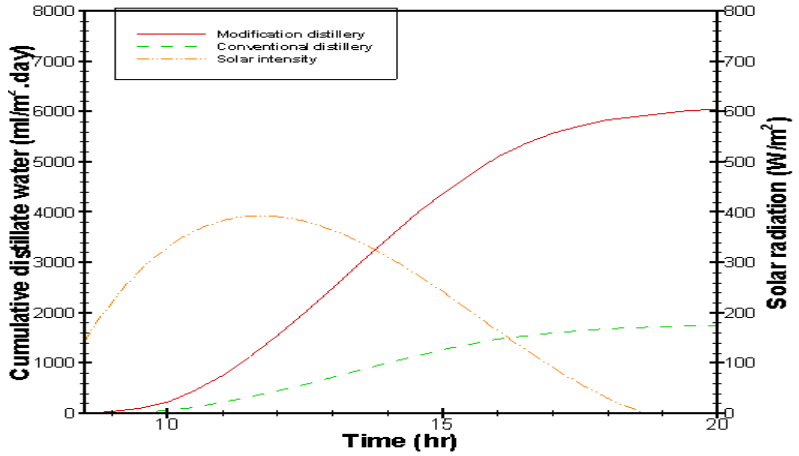

Fig. (18). Variation of theoretical solar radiation intensity and amount of cumulative distillate water for the conventional and modified solar still with time of the day on Feb. 16. 2018.

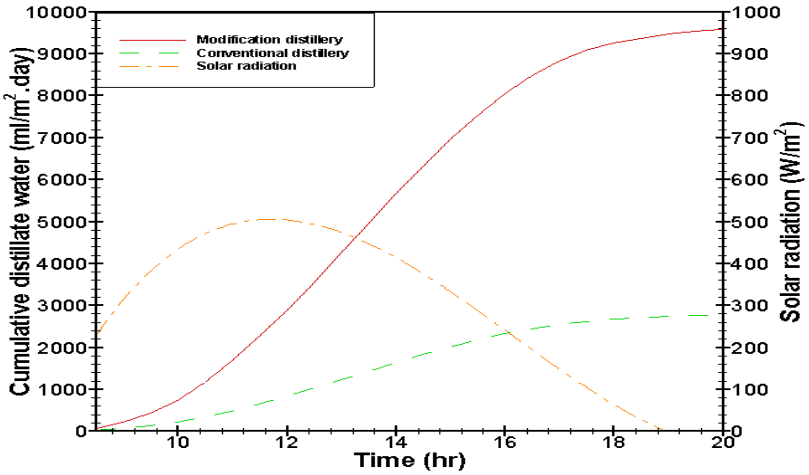

Fig. (19). Variation of theoretical solar radiation intensity and amount of cumulative distillate water for the conventional and modified solar still with time of the day on Mar. 16. 2018.

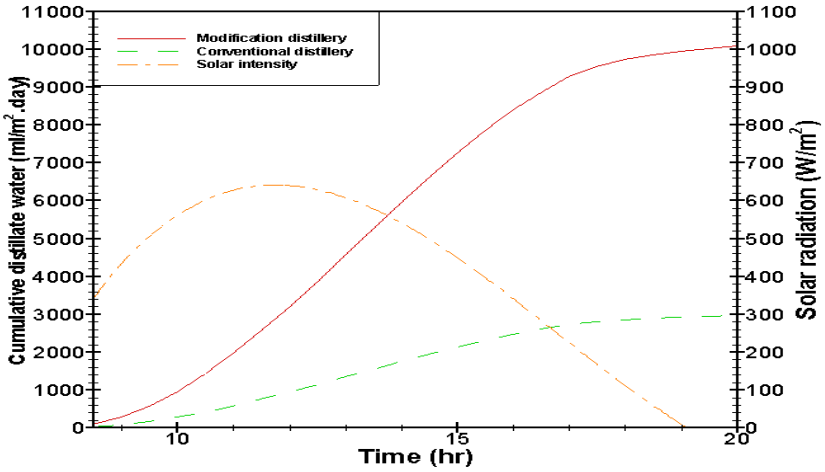

Fig. (20). Variation of theoretical solar radiation intensity and amount of cumulative distillate water for the conventional and modified solar still with time of the day on Apr. 15. 2018.

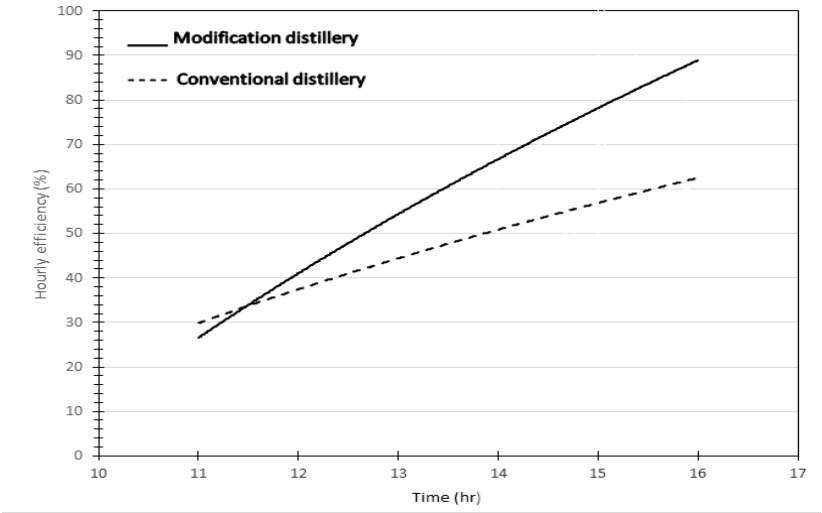

Fig. (21). Variation of hourly efficiency for the conventional and modified solar still on Jan. 17. 2018, Kirkuk, Iraq.

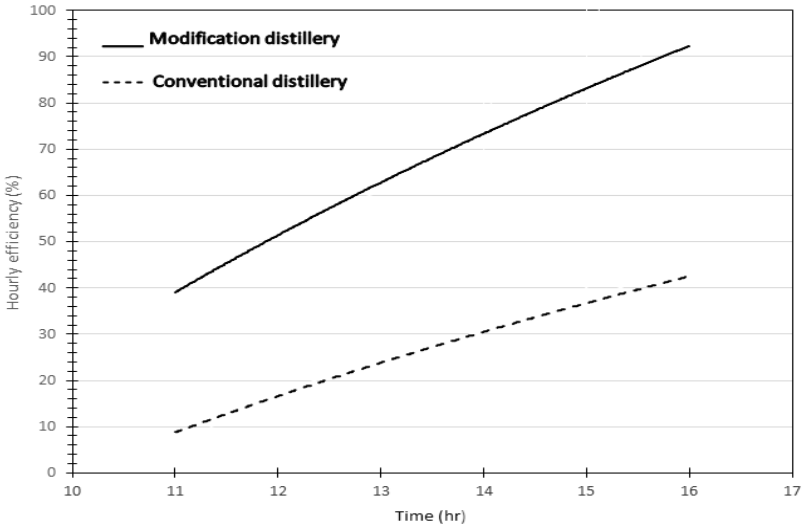

Fig. (22). Variation of hourly efficiency for the conventional and modified solar still on Feb. 16. 2018, Kirkuk, Iraq.

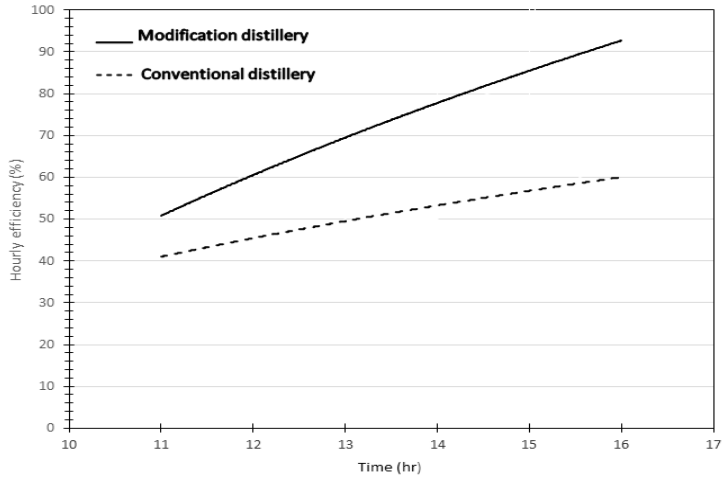

Fig. (23). Variation of hourly efficiency for the conventional and modified solar still on Mar. 16. 2018, Kirkuk, Iraq.

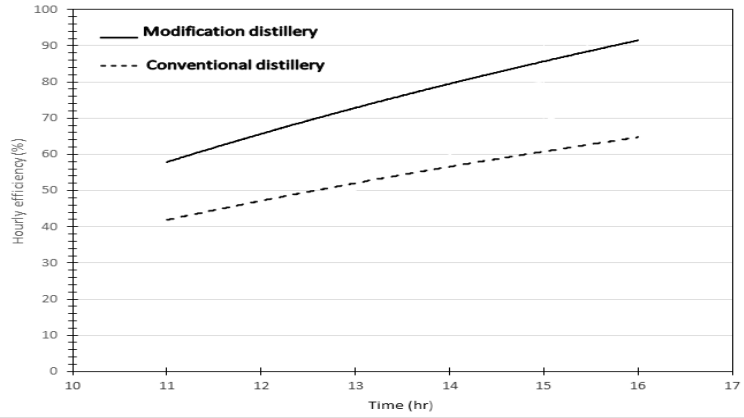

Fig. (24). Variation of hourly efficiency for the conventional and modified solar still on Apr. 15. 2018, Kirkuk, Iraq.

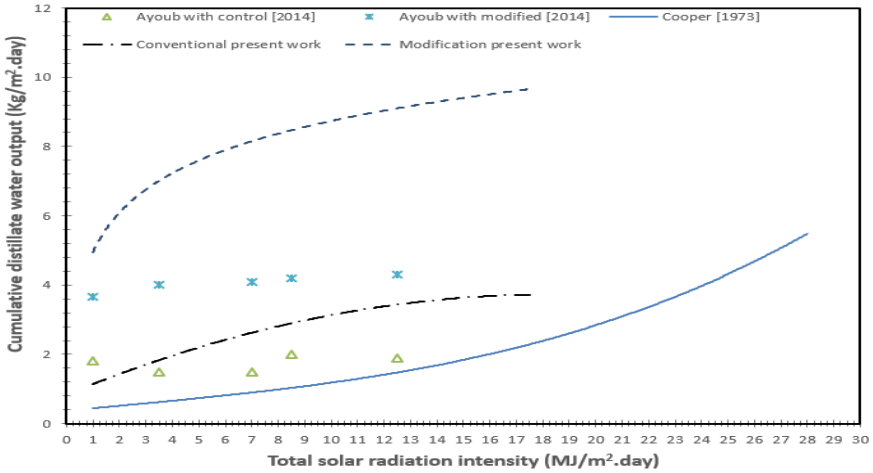

Fig. (25). The variation of daily cumulative distillate water output for different types of solar still with total solar radiation intensity, 2018, Kirkuk, Iraq.

REFERENCES

M.A.S. Malik, G.N. Tiwari, A. Kumar and M.S. Sodha, "Solar Distillation", Pergamon Press, Oxford, (1985).

Bhanu Pratap Singh, "Performance evaluation of an integrated single slope solar still with solar water heater", MIT International Journal of Mechanical Engineering Vol. 1, ISSN: 2230 – 7699, pp.: 68-71, (2011).

Omar Badran, "Theoretical analysis of solar distillation using active solar still", International Journal of Thermal & Environmental Engineering, Vol. 3, No. 2, pp.: 113-120, (2011).

Lilian Malaeb , Kamel Aboughali and George M. Ayoub, "Modeling of a modified solar still system with enhanced productivity ", Solar Energy 125, PP.: 360–372, (2016).

Incropera, Dewitt, Bergman and Lavine, "Fundamentals of heat and mass transfer", Sixth Edition, www.wiley.com, (2005).

D. W. Medugu and L. G. Ndatuwong, "Theoretical analysis of water distillation using solar still", International Journal of Physical Sciences, Vol. 4, No. 11, pp.: 705-712, (2009).

Jose L. Fernandez and Norberto Chargoy, "Multi-stage, indirectly heated solar still", Solar Energy, Vol. 44, No. 4, pp.: 215-223, (1990).

P.T. Tsilingiris, "Thermophysical and transport properties of humid air at temperature range between 0 and 100 ^{o}C", Energy Conversion and Management, Vol. 49, pp.: 1098–1110, (2008).

John A. Duffie and William A. Beckman, "Solar engineering of thermal processes", Second Edition, (1980).

S. Tharmalingam and W. L. Wilkinson, "The coating of Newtonian liquids on to a rotating roll", Chemical Engineering Science, Vol. 33, pp.: 1481-1487, (1978).

A.E. Kabeel and Mohamed Abdelgaied, "Improving the performance of solar still by using PCM as a thermal storage medium under Egyptian conditions", Desalination Vol. 383, pp.: 22–28, (2016).

Muafag Suleiman K. Tarawneh, "Effect of water depth on the performance evaluation of solar still", Jordan Journal of Mechanical and Industrial Engineering, Vol. 1, No. 1, pp.: 23 - 29, (2007).

Bilal A. Akash, Mousa S. Mohsen and Waleed Nayfeh, "Experimental study of the basin type solar still under local climate conditions", Energy Conversion & Management 41, pp.: 883–890, (2000).

A.K. Sethi and V.K. Dwivedi, "Exergy analysis of double slope active solar still under forced circulation mode", Desalination and Water Treatment, Vol. 51, pp.: 7394-7400, (2013).

P. I. Cooper, "The Maximum Efficiency of Single Effect Solar Stills", Solar Energy, Vol. 15, pp.: 205-217, (1973).

George M. Ayoub and Lilian Malaeb, "Economic Feasibility of a Solar Still Desalination System with Enhanced Productivity", Desalination, Vol. 335, pp.: 27–32, (2014).